حوزه انجمن های علمی دانشجویی
دانشگاه پیام نور مرکز اصفهان
کنفرانس دانشجویی
یافته های زیست-پزشکی نوین ایران
1nd Conference on Modern Bio-Medical Researches

The Study of Fluorescent Carbon Dots for Fabrication of Biocompatible Gelatin Nanomaterials

Sina Afshari [1], Rahman Saeidi [1], Iman Yazdanpanah[1], Saman Raofi [1], Ahmad Riahi [2]

[1] Polymer Research Laboratory, Department of Organic and Biochemistry, Faculty of Chemistry, University of Tabriz, Tabriz, Iran.

[2] Department of Biology, Payam Noor University, Tehran, Iran

*corresponding author : hesamsoh1395@gmail.com

ABSTRACT

In recent years, fluorescent carbon dots (CDs) have attracted a great deal of attention in imaging and related biomedical applications due to their excellent photoluminescence properties, low cost, high quantum yield and low cytotoxicity in comparison with semiconductor quantum dots based on metallic elements. In this paper, a new design for development of CDs/gelatin nanoparticles (CDs/GNPs) is described. The obtained fluorescent nanocarriers were characterized using FT-IR, SEM, XRD, DLS, PL analysis. Afterwards, the performance of developed NPs was investigated through different in-vitro tests such as MTT assay, fluorescence microscopy analyses. Methotrexate (MTX) was successfully loaded into the fluorescent NPs at physiological pH (7.4) by ionic interactions between anionic carboxylate groups of MTX and cationic amino groups on the surface of NPs. The MTT assay revealed that the MTX-loaded nanocarriers have higher cytotoxicity in MCF-7 breast cancer cells than nanocarriers without MTX. Upon the obtained results, our fluorescent nanocarriers hold great potential as drug carriers for the targeted MTX delivery to the cancer cells and biological fluorescent labelling.

Keywords: Carbon Dots, Gelatin Nanoparticles, Cell imaging, Methotrexate

1. INTRODUCTION

Recent years, fluorescent nanomaterials have gained greater attention owing to their unique optical properties and a wide range of potential in medical applications [1-3]. Up to now, different types of fluorescent nanomaterials such as semiconductor quantum dots, polymer dots, carbon nanodots and liposome fluorescent nanomaterials have been synthesized and studied in various applications [4-6]. By comparing semiconductor quantum dots (QDs) based on metallic elements, such as PbSe, CdSe, CdS, and Ag_2S with fluorescent carbon-based nanodots (CDs), CDs are the excellent fluorescent nanomaterials due to their good biocompatibility, easy to modify, and low toxicity biocompatibility [7]. So, CDs were used as promising materials for various applications such as gene transmission, bioimaging, biosensing, disease detection and drug delivery [8-10]. Moreover, to develop these fluorescent nanoparticles (NPs) with effective drug delivery systems, the use of natural biopolymeric nanocarriers can be proposed to load of these fluorescent materials [11, 12]. Among the natural biopolymers, gelatin is one of the desirable materials used in foodstuff, pharmaceutical, cosmetic and medical applications due to its excellent biodegradability and biocompatibility. Furthermore, gelatin is a non-toxic and natural polyampholyte biopolymer gained either by partial acid (type-A) or alkaline (type-B) hydrolysis of collagen [13-15]. In general, gelatin-based NPs (GNPs) are considered as a useful biomaterial nanocarrier for drugs and bioactive molecules because of its excellent surface chemical modification potential and cross-linking possibility. The complex of fluorescent nanodots/GNPs showed potential applications in drug delivery and bioimaging, simultaneously. In this regard, several works have been studied and reported for fluorescent GNPs [16-18]. However, the toxicity of QDs may hold back their *in-vivo* applications due to the direct release of cytotoxic metals of QDs into the biological system which could damage normal cells because of severe toxicity [19-21]. Thus, to overcome this problem, CDs can be used as a fluorescent dye with excellent biocompatibility and easy combination with natural biopolymer nanocarrier. As we know, no previous investigations have been reported about the synthesis of CDs embedded GNPs. Methotrexate

(MTX) is one of the most widely used therapeutic agents to treat various cancers such as breast cancer, choriocarcinoma, lung cancer and bladder carcinoma [22-24]. Moreover, MTX has structural similarity with folic acid (FA) which would be able to enter cells through a similar transport system of FA as a targeting ligand on the surface of cancer cells [25-27]. Thus, in this paper, we report the preparation of fluorescent GNPs with the loading of MTX on the surface of NPs as a targeting and therapeutic agent. In the first step, CDs with an excellent fluorescence quantum yield of 75% were prepared by the one-step hydrothermal method process [28]. Then, CDs/GNPs were synthesized via two-step dissolution method. Then, MTX as a model drug was loaded on the surface of nanocarriers via ionic interaction between nanocarrier and drug. Finally, MTT assay and cellular uptake were performed on the breast cancer cell line (MCF-7) for investigation of MTX-loaded nanocarrier cytotoxicity effects.

2. Materials and methods

2.1 Materials

Type A gelatin (300 Bloom) was supplied from Sigma-Aldrich Co. (Missouri, USA). Citric acid and polyethylene glycol (PEG-2000), ethylenediamine, glutaraldehyde (25% v/v aqueous solution), acetone and dimethyl sulfoxide (DMSO) were procured from Merck Chemicals Co. Methotrexate salt (MTX) was obtained from Zahravi Pharmaceutical Co. (Tabriz, Iran). Breast carcinoma cell line (MCF-7) was bought from the Iranian Blood Transfusion Institute. All reactants possessed analytical grade and deionized (DI) water was used throughout the work.

2.2 Characterization

Structural and Morphological analyses of the CDs/GNPs complexes were imaged with a field emission scanning electron microscope (FE-SEM) system (MIRA3 FEG-SEM, Tescan, Czech), for this purpose, samples were dispersed and sonicated in DI water. Functional groups of the samples were detected with a Tensor 27 FTIR spectrophotometer (Bruker, Germany) using KBr pellets. X-ray diffraction (XRD, Bruker D-8, Germany) was recorded using Cu Kα radiation in the 2θ ranges of 10- 60° to determine the crystal structure. The Ultraviolet-visible (UV-Vis) (UV-2550 UV– vis spectrophotometer, Shimadzu, Japan) absorption spectra were recorded at ambient temperature using DI water as the blank. The characteristics photoluminescence (PL) emission spectra of fluorescent GNPs were recorded by a fluorescence spectrophotometer (LS45, PerkinElmer).

2.3 Synthesis of Carbon dots (CDs)

CDs were formulated using a one-step hydrothermal reaction following a previously reported [28]. In brief, a mixture of 4 g citric acid and 0.8 g PEG-2000 were added to 30 ml DI water followed by addition of 8 ml ethylenediamine. The mixture slightly stirred until a clear homogeneous solution acquired. After that, the mixture was poured into a 100 mL Teflon tank. Next, the Teflon tank was sealed in a stainless steel autoclave and heated at 160 °C for 8 hrs. Finally, the reactor was naturally cooled down to ambient temperature. In order to remove the large particles, the resulting red-brown solution was centrifuged at 12000 rpm for 15 min. Then, the supernatant liquor was further purified in a dialysis bag (MWCO = 12000 Da, Sigma-Aldrich, USA) against of DI water for 24 hrs to remove small molecule substances. The quantum yield of synthesized CDs was calculated to be approximately 75% according to the reported method.

2.4 Synthesis of CDs/gelatin nanoparticles (CDs/GNPs)

The fluorescent GNPs were synthesized by the two-step desolvation method [29]. Briefly, 25 ml of 5% gelatin solution was prepared at 50 °C. After the solution cooled down to ambient temperature, an equal volume of acetone was added to precipitate the high molecular weight (HMW) gelatin. Then, the HMW gelatin was dissolved in 25 ml DI water and stirring under constant heating. The as-prepared CDs solution (10.0 mL) was added to the gelatin mixture at this point. Acetone was added (dropwise) to the solution to form fluorescent GNPs. Then, the mixture was cross -linked with 200 µL glutaraldehyde solution overnight at room temperature to stabilize the NPs. The fluorescent GNPs were then purified by a three-fold centrifugation at 10000 rpm for 15 min to remove the acetone and excess free cross-linker and CDs. The resultant NPs were stored at 4 °C. The powder of fluorescent GNPs was obtained by lyophilization. Fig. 1 presents schematically the preparation of fluorescent GNPs.

2.5 *In Vitro* cell cytotoxicity

The cytotoxicity and the biocompatibility tests of the NPs were evaluated by comparing the free MTX, MTXCDs/GNPs and CDs/GNPs (Without MTX) with MTT Assay. MCF-7 cells at a density of 2×10^4 cells per well in RPMI 1640 medium were seeded into a 96-well plate and incubated overnight at 37 °C in 5% CO_2 atmosphere. After that, the cells were treated with various concentrations of free MTX, MTX-CDs/GNPs, and CDs/GNPs and incubated for 48 hrs. Then, the MTT solution (5 mg/mL) was added to the wells and stored for further 4 hrs. After aspiration of the medium, MTT-formation was dissolved in 200 µl of DMSO, and the optical density (OD) was recorded by a microplate reader (Elx808, Biotek, USA) at 570 nm.

2.6 *In vitro* cell imaging studies

MCF-7 cells were performed to investigate the potential capability of CDs/GNPs for cell imaging. The fluorescence imaging of cells treated with CDs/GNPs and MTX-CDs/GNPs was shown in Figure. 5. The cells were seeded onto glass coverslips placed in six-well plates and cultured in RPMI 1640 medium containing 10% fetal bovine serum in a 5% CO_2 environment. After 24 hrs, the medium was removed from each well and the seeded cells were washed with PBS buffer (pH 7.4). Then, 2 mL aliquots of CDs/GNPs and MTX-CDs/GNPs (10 µg mL^{-1}) in PBS were added to the cell culture medium followed by 3h culture at 37 °C in a 5% CO_2 environment. The coverslips were put onto the glass microscope slides and the typical photographs were captured from stained cells using an inverted fluorescence microscopy (Olympus, Bh2-RFCA, Japan).

3. Results and Discussion

3.1 Synthesis of fluorescent nanocarrier

In this study, we have designed the fluorescent nanocarriers for anticancer drug delivery from the perspective of in vitro cellular imaging by incorporating CDs as presented in Figure.1. To prepare the fluorescent nanocarriers, first biocompatible CDs were synthesized by a one-step hydrothermal treatment. Then these prepared CDs were inserted into the GNPs by the two-step desolvation method. The developed NPs can be coupled interacted via electrostatic interaction between amino groups of gelatin NPs and carboxylic groups on the surface of CDs.

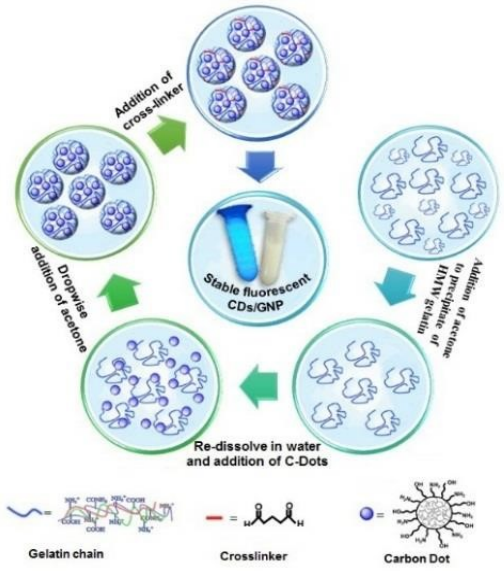

Fig. 1. *Schematic illustration of the fluorescent GNP synthesis via two-step desolvation method.*

3.2 Spectral characterization of the Fluorescent nanocarrier

The UV–Vis absorption and PL spectra of the CDs/GNPs were recorded and compared to CDs. PL studies show the aqueous solution of CDs/GNPs emits strong blue light under excitation with a UV lamp at 365 nm and the PL intensity of NPs was stable after storage for 30 days in the dark. The UV-vis absorption wavelength of the CDs/GNPs was found to have no significant change compared with free CDs as shown in Figure. 2a. Similar to the one previously reported in the literature UV-Vis spectrum of the fluorescent GNPs have two peaks, one at 250 nm and a broad absorption band at around 350 nm corresponding to the π-π* transition of sp^2 domains and n-π*

transition of multiconjugate C=O of the CDs, respectively [28]. The maximum PL emission peak is found at 450 nm for CDs when excited at 360 nm. However, the PL emission peaks of the CDs/GNPs moved to longer wavelengths (red-shifted from 450 to 460 nm) (Figure. 2b). This may be probably due to the entrapment of CDs into the gelatin matrix and the distance between two CDs reduces due to the electrostatic attraction between the negatively charged CDs and positively charged protein that increases the dipole-dipole interaction between CDs resulting in a red shift in the fluorescence spectrum [31, 32].

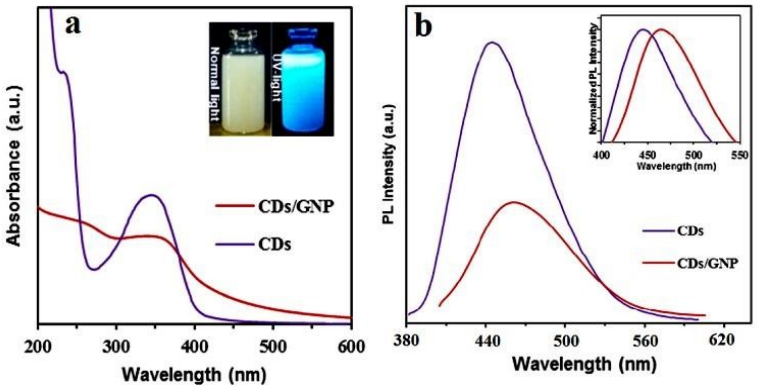

Fig. 2. *UV-vis absorption (a), PL spectra and normalized PL emission (b) of CDs and CDs/GNPs.*

3.3 FT-IR analysis

Figure. 3 shows FTIR spectra of synthesized GNPs (a), CDs (b) and CDs/GNPs (c). C=O stretching can be observed in both GNP and CDs occurring around ~1650 cm^{-1}. In the FTIR spectra of GNPs, the characterization absorption band at 3354 cm^{-1} is related to the stretching vibration of N-H and O-H bonds. Also, the stretching vibration of C-H bonds appeared at 2940 cm^{-1}. A stronger peak at 1450 cm^{-1} is related to the aldimine linkage (CH=N) is formed by the reaction of the aldehyde group of glutaraldehyde as the crosslinking agent with the amino group of gelatin protein backbone [33]. The FTIR spectrum of CDs shows broad peaks from 3000 to 3400 cm^{-1} due to the stretching vibrations of -OH groups. The stretching and bending the vibrations of -CH2- is observed according to the distinctive peaks at 2943 and 1450 cm^{-1} separately. The characteristic absorption bands at 1702 and 1242 cm^{-1} related to the stretching vibrations of C=O and C-O groups, demonstrating the existence of the ester bond. The amide bond is confirmed by the typical peaks centered at 1647 and 1350 cm^{-1} contributed to the frequency of the vibrations of C=O and C-N, respectively. The two peaks at 840 and 1110 cm^{-1} corresponded to the symmetrical and asymmetrical stretching vibrations of C-O-C groups [28]. Also, most of the characteristic peaks of CDs and GNPs (stretches of -C=O, -CH2 and -OH groups) are observable in CDs/GNPs. A blue shift and decrease intensity of vibration frequencies of carbonyl groups were observed in CDs/GNPs, which might be due to electron cloud between carbon, and oxygen atoms moved to the direction of oxygen [34, 35].

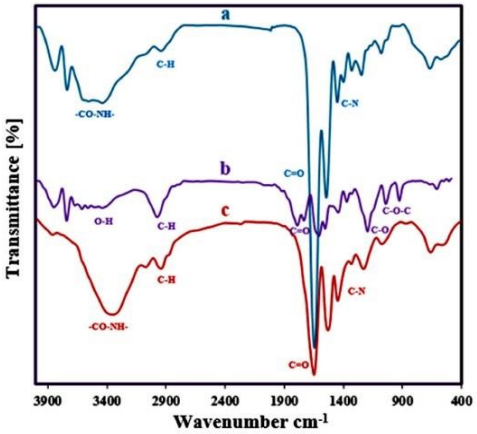

Fig. 3. *FTIR spectra of GNPs (a), CDs (b) and CDs/GNPs (c).*

3.4 Morphological and structural characteristic

The morphology, size and zeta potential (ZP) of CDs/GNPs are displayed in Figure. 4. The morphologies of the prepared NPs using freeze-drying are clearly illustrated by SEM. SEM images were shown the uniformity in the shape and size of the prepared NPs, as well. The average size of dispersing CDs/GNPs was around 35±5 nm. This size of the NPs is actually between the favored ranges of effective drug delivery [39]. The average hydrodynamic size of the aqueous suspension of NPs was determined by DLS measurement is shown in Figure. 4c. The obtained result revealed that the hydrodynamic size of the NPs is 100-200 nm. Due to the aggregation of NPs and undergo a swelling process in aqueous medium 40, the size distribution obtained from DLS technique is a larger than the particle size acquired from SEM. The XRD technique was employed to determine the phase formation and the crystallization of synthesized NPs

(Figure. 4d). The broad peaks observed in the XRD patterns of GNP and CDs/GNPs around at $2\theta = 22.5°$ representing poor crystallinity in gelatin and amorphous carbon phase in CDs [35].

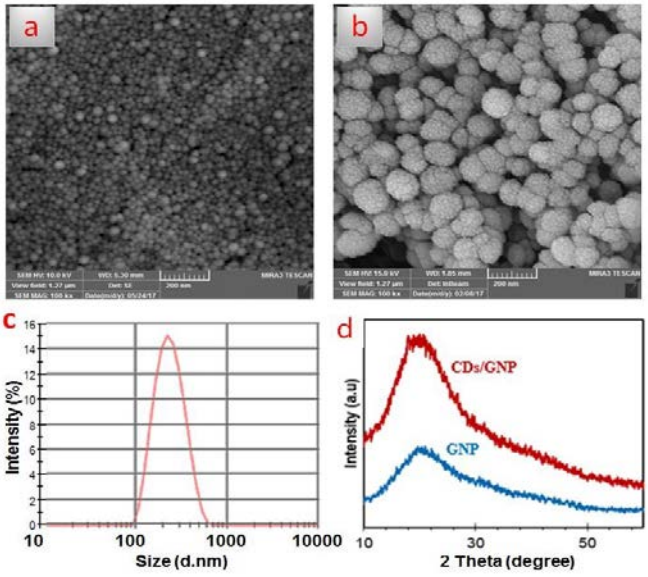

Fig. 4. *SEM images of CDs/GNPs before freeze-drying (a) and after freeze-drying (b). Size profiles (c) of the CDs/GNPs. XRD patterns (d) for GNPs, and CDs/GNPs.*

3.5 In vitro cytotoxicity study

To explore the biocompatibility of developed nanocarrier and anticancer activity of MTX-loaded nanocarrier, MTT cell assays were performed against the MCF-7 breast cancer cell line. In comparing the cytotoxicity results of the free form of MTX with MTX loaded CDs/GNPs, the drug-loaded nanocarriers showed higher cell cytotoxicity than free MTX for 48 hrs (Figure. 5a). Furthermore, to confirm the cell cytotoxicity of MTX-CDs/GNPs as a potent drug delivery system, the biocompatibility of nanocarrier (without MTX) was first studied and exhibited no obvious cytotoxicity for blank nanocarrier in MCF-7 cells after 48 hrs, confirming that the nanocarrier presented good biocompatibility. Finally, these results would be invaluable in escaping the dose-dependent side effects of MTX drug.

3.6 In vitro bioimaging study

The bioimaging applications of the CDs/GNPs were examined based on the excellent fluorescence properties of the CDs coupled to the nanocarriers. As shown in Figure. 5b, after the CDs/GNPs were incubated with MCF-7 cells for 3 hrs, the fluorescence images of the cells were taken using a fluorescence microscope invert, confirming that the CDs/GNPs have a potential for bioimaging applications. On the other hand, the MCF-7 cells incubated with MTXCDs/GNPs and showed strong blue color rather than nanocarriers without MTX which is due to the similar structure of MTX to folic acid and the presence of folic acid receptor on the surface of MCF-7 cells [44, 45].

Therefore, we could prove the presence of MTX on the surface of developed nanocarriers and showed a good agreement with my hypothesis and design.

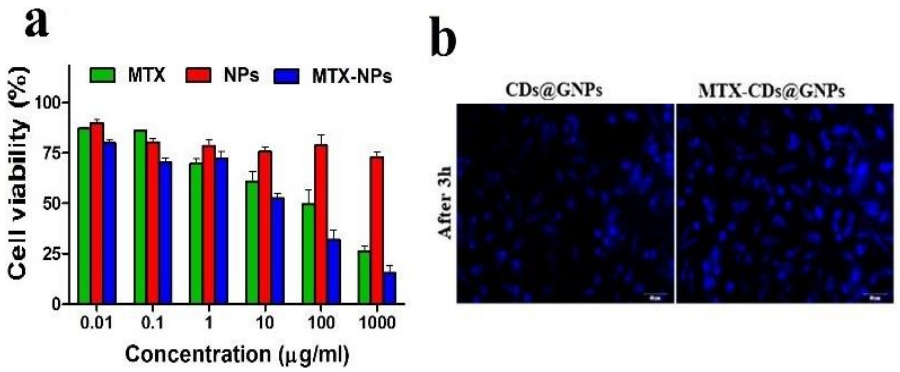

Fig. 5. *Cell viability of MTX, CDs/GNPs, and MTX loaded CDs/GNPs at various concentrations versus breast cancer (MCF-7) cell line for 48 hrs (a), and Fluorescence microscopy images of treated human breast epithelial adenocarcinoma (MCF-7) cells with CDs/GNPs and treatment with MTX-CDs/GNPs after for 3h (All scale bars are 50µm) (b).*

4. Conclusion

In this report, we designed a biocompatible fluorescent gelatin nanoparticle (CDs/GNP) as a newly developed nanocarrier for in vitro cell imaging and MTX delivery. First, the CDs/GNPs were successfully prepared via the twostep dissolution method. The nanoparticles display bright blue light under a UV lamp and show good stability. Second, MTX-loaded nanocarrier was prepared. The ionic interaction between the NPs and MTX are responsible for loading content of anticancer drug molecules. The MTT assay results indicated that NPs are highly biocompatible and MTXloaded nanocarrier exposed a high cytotoxicity in MCF-7 breast cancer cell in comparison to frees drugs. Also, the successful cell internalization of MTX-loaded nanocarrier was quantitatively validated by the use of cellular uptake studies. These results indicated that the developed fluorescent nanocarrier could be used as a promising candidate for applications in bio-imaging and effectively used as an efficient targeted delivery of MTX to cancer tissues and also can be used for further *in-vivo* applications.

REFERENCES

1. Mehdi Kargarfard, R.R., Ayeh Rizvandi, Mehdi Dahghani, Parinaz Poursafa, Hemodynamic physiological response to acute exposure to air pollution in young adults according to the fitness level. ARYA Atherosclerosis, 2009. 5(3).

2. Rizvandi, A., et al., The Evaluation of Performance Indicators of Coaches in Football Development. Journal of Humanities Insights, 2019. 03(04): p. 248-254.

3. Aye Rizvandi, M.T.G., Mohammadreza Esmaeili, Farideh Ashraf Ganjoee, The Evaluation of Performance Indicators of Coaches in Football Development. Journal of Humanities Insights, 2019. 3(4).

4. Aye Rizvandi, F.T., Zahea Sadegh Zadeh, Sport consumer behaviour model: Motivators and constraints. Universidad de Alicante. Área de Educación Física y Deporte, 2019. 14.

5. Aye Rizvandi, F.T., Entrepreneurial marketing effects on sport club manager performance (Conceptual Model). Universidad de Alicante. Área de Educación Física y Deporte, 2019. 14.

6. Aye Rizvandi, M.F., Maryam Asadollahi Supply Chain Management for Sporting Goods Retailing. 2020: Mikima Book Publication.

7. Narmin Najafzadeh, M.M.S., Syed Shuja Sultan, Adel Spotin, Alireza Zamani, Roozbeh Taslimian, Amir Yaghoubinezhad, Parviz Parvizi, The existence of only one haplotype of Leishmania major in the main and potential reservoir hosts of zoonotic cutaneous leishmaniasis using different molecular markers in a focal area in Iran. Revista da Sociedade Brasileira de Medicina Tropical, 2014. 47(5).

8. Adel Spotin, S.R., Parviz Parvizi, Parnazsadat Ghaemmaghami, Ali Haghighi, Aref Amirkhani, Ali Bordbar, Amir Yaghoubinezhad, Different Phenotypic Aspects with No Genotypic Heterogeneity in Leishmania Major Isolates of Suspected Patients in Northern Khuzestan Province. Iranian Journal of Public Health, 2014. 43(2).

9. Neda Samei, P.P., Adel Spotin, Mohammad Reza Khatami Nezhad, Narmin Najafzadeh, Amir Yaghoubinezhad, IDENTIFYING OF CAUSATIVE AGENTS OF CUTANEOUS LEISHMANIASES BY AMPLIFYING CYT B GENE IN INDIGENOUS FOCI OF Iran. Iranian Journal of Public Health, 2014. 43(2).

10. Neda Samei, P.P., Mohammadreza Khatami Nezhad, Amir Yaghoubinezhad, Narmin Najafzadeh, Adel Spotin, Finding various molecular haplotypes of Leishmania major in human using three HSp70, ITS-rDNA and Cyt b genes, in 1st and 13th Iranian Genetics Congress. 2014: Tehran.

11. Somayyeh Heidary, A.Y.N., Atefeh Mehrabi Far, Colonization and Investigation of Vibrio Cholera Recombination Protein in E-Coli. International Journal of Engineering & Technology, 2018. 7(4.7).

12. Mostafavi, S.M., et al. Electrochemical Study and Determination of Thiophene by Cobalt Oxide Nanoparticle Modified Glassy Carbon Electrode. in 6th Aegean Analytical Chemistry Days (AACD), Denizli, Turkey. 2008.

13. Seyed Mojtaba Mostafavi, S.A., Iman Seyedi, Mohammad Hoseini, Excel for Engineers. 2009, Toranj Group Publication, Ltd.

14. Seyed Mojtaba Mostafavi, A.R., Masoumeh Piryaei, Electrochemistry : principles, methods, and applications. 2009, Toranj Group Publication, Ltd.

15. Seyed Mojtaba Mostafavi, A.M., Determination of molecular structure by identification of functional groups. 2010, Toranj Group Publication, Ltd., Isfahan, Iran.

16. Seyed Mojtaba Mostafavi, O.Z., Thermodynamics: an engineering approach. 2010, Mani Publication, Ltd, Isfahan, Iran.

17. Seyed Mojtaba Mostafavi, B.R., Nanomaterial Chemistry. 2010, Toranj Group Publication, Ltd.

18. Zabihi, O., et al., The effect of zinc oxide nanoparticles on thermo-physical properties of diglycidyl ether of bisphenol A/2, 2′-Diamino-1, 1′-binaphthalene nanocomposites. Thermochimica acta, 2011. 521(1-2): p. 49-58.

19. Seyed Mojtaba Mostafavi, A.R., Mina Adibi, Farshid Pashaee, Masoumeh Piryaei, Modification of Glassy Carbon Electrode by a Simple, Inexpensive and Fast Method Using an Ionic Liquid Based on Immidazolium as Working Electrode in Electrochemical Determination of Some Biological Compounds. Asian Journal of Chemistry, 2011. 23(12).

20. Seyed Mojtaba Mostafavi, A.R., Mina Adibi, Farshid Pashaee, Masoumeh Piryaei, Electrochemical Investigation of Thiophene on Glassy Carbon Electrode and Quantitative Determination of it in Simulated Oil Solution by Differential Pulse Voltammetry and Amperometry Techniques. Asian Journal of Chemistry, 2011. 23(12): p. 5356-5360.

21. Zabihi, O., A. Khodabandeh, and S.M. Mostafavi, Preparation, optimization and thermal characterization of a novel conductive thermoset nanocomposite containing polythiophene nanoparticles using dynamic thermal analysis. Polymer degradation and stability, 2012. 97(1): p. 3-13.

22. Shamsipur, M., et al., Biotransformation of methyl tert-butyl ether by human cytochrome P450 2A6. Biodegradation, 2012. 23(2): p. 311-318.

23. Seyed Mojtaba Mostafavi, A.R., Ali Akbar Miranbeigi, Handbook of Mineral Analysis. 2012, Mani Publication, Ltd, Isfahan, Iran.

24. Seyed Mojtaba Mostafavi, M.P., Ahmad Rouhollahi and A. Mohajeri, Separation and Quantification of Hydrocarbons of LPG Using Novel MWCNT-Silica Gel Nanocomposite as Packed Column Adsorbent of Gas Chromatography. Journal of NanoAnalysis, 2014. 1(01): p. 01.

25. Seyed Mojtaba Mostafavi, M.P., Ahmad Rouhollahi and A. Mohajeri, Separation of Aromatic and Alcoholic Mixtures using Novel MWCNT-Silica Gel Nanocomposite as an Adsorbent in Gas Chromatography. Journal of NanoAnalysis, 2014. 1(01): p. 11.

26. Mostafavi, S.M., 3D Graphene Biocatalysts for Development of Enzymatic Biofuel Cells: A Short Review. Journal of Nanoanalysis, 2015. 2(2): p. 57-62.

27. Parvanian, S., S.M. Mostafavi, and M. Aghashiri, Multifunctional Nanoparticle Developments in Cancer Diagnosis and Treatmen. Sensing and Bio-Sensing Research, 2016. 1(2): p. 22.

28. Mostafavi, S.M. Enhancement of mechanical performance of polymer nanocomposites using ZnO nanoparticles. in 5th International Conference on Composites: Characterization, Fabrication and Application (CCFA-5). 2016. Iran University of Science and Technology.

29. Abolfazl Davoudiroknabadi, S.M.M., Seyed Sajad Sajadikhah, An Introduction to Nanotechnology. 2016, Mikima Book.

30. Abolfazl Davodiroknabadi, S.M.M., Ali Asghar Pasban, Fundamentals of Nanostructure and Nanomaterial. 2016, Mikima Book.

31. Pasban, A., et al., Quantitative Determination of LPG Hydrocarbons by Modified Packed Column Adsorbent of Gas Chromatography Via Full Factorial Design. Journal of Nanoanalysis, 2017. 4(1): p. 31-40.

32. Somayyeh Heidari, M.I., Seyed Mojtaba Mostafavi, , A Validated and Rapid HPLC Method for Quantification of Human Serum Albumin in Interferon beta-1a Biopharmaceutical Formulation. MedBioTech Journal, 2017. 1(01): p. 29.

33. Mostafavi, S.M., K. Bagherzadeh, and M. Amanlou, A new attempt to introduce efficient inhibitors for Caspas-9 according to structure-based Pharmacophore Screening strategy and Molecular Dynamics Simulations. Medbiotech Journal, 2017. 01(01): p. 1-8.

34. Amanlou, M. and S.M. Mostafavi, In sillico screening to aim computational efficient inhibitors of caspase-9 by ligand-based pharmacophore modeling. Medbiotech Journal, 2017. 01(01): p. 34-41.

35. Mostafavi, S.M., et al., Acidity removal of Iranian heavy crude oils by nanofluid demulsifier: An experimental investigation. Journal of Nanoanalysis, 2017: p. 10-17.

36. Aida Badamchi Shabestari, B.A.A., Maryam Shekarchi, Seyed Mojtaba Mostafavi, Development of Environmental Analysis for Determination of Total Mercury in Fish Oil Pearls by Microwave Closed Vessels Digestion Coupled with ICP-OES. Ekoloji, 2018. 27(106): p. 1935.

37. Bayat, M. and S.M. Mostafavi, Investigation of Interleukin 2 as Signaling Molecule in Human Serum Albumin. The Pharmaceutical and Chemical Journal, 2018. 5(02): p. 183-189.

38. Samira Eissazadeh, S.M.M., Masoumeh Piryaei, and M.S. Taskhiri, Application Of Polyaniline Nanostructure Based Biosensor For Glucose And Cholesterol Detection. Research Journal of Pharmaceutical, Biological and Chemical Sciences, 2019. 10(1): p. 150.

39. Samira Eissazadeh, M.P., Mohammad Sadegh Taskhiri and S.M. Mostafavi, Improvement of Sensitivity of Antigen-Antibody Detection of Semen Through Gold Nanoparticle. Research Journal of Pharmaceutical, Biological and Chemical Sciences, 2019. 10(1): p. 144.

40. Samira Eissazadeh, M.P. and S.M. Mostafavi, Measurement of Some Amino Acid Using Biosensors Based on Silicon-Based Carbon Nanotubes. Journal of Computational and Theoretical Nanoscience, 2019. 16: p. 1.

41. Aida Badamchi Shabestari, S.M.M., Hanieh Malekzadeh, Force Degradation Comparative Study on Biosimilar Adalimumab and Humira. Revista Latinoamericana de Hipertensión, 2019. 13(06): p. 496-509.

42. Mostafavi, S.M., S. Eissazadeh, and M. Piryaei, Comparison of Polymer and Ceramic Membrane in the Separation of Proteins in Aqueous Solution Through Liquid Chromatography. Journal of Computational and Theoretical Nanoscience, 2019. 16(1): p. 157-164.

43. Ahmadipour, A., P. Shaibani, and S.A. Mostafavi, Assessment of empirical methods for estimating potential evapotranspiration in Zabol Synoptic Station by REF-ET model. Medbiotech Journal, 2019. 03(01): p. 1-4.

44. Jafari, S. and S.A. Mostafavi, Investigation of nitrogen contamination of important subterranean water in the plain. Medbiotech Journal, 2019. 03(01): p. 10-12.

45. Z. Man, A.G.E., S. M. Mostafavi, A. Surendar, Fuel oil characteristics and applications: economic and technological aspects. Petroleum Science and Technology, 2019.

46. Seyed Mojtaba Mostafavi1, H.M. and M.S. Taskhiri, In Silico Prediction of Gas Chromatographic Retention Time of Some Organic Compounds on the Modified Carbon Nanotube Capillary Column. Journal of Computational and Theoretical Nanoscience, 2019. 16(01): p. 151-156.

47. Mostafavi, S.M. and A. Ebrahimi, Mercury determination in work place air and human biological samples based on dispersive liquid-liquid micro-extraction coupled with cold vapor atomic absorption spectrometry. Analytical Methods in Environmental Chemistry Journal, 2019. 2(04): p. 49-58.

48. Anbia, M., et al., Employing a new modified nanoporous carbon for extraction and determination of 1,10-phenanthroline and 2,2′-bipyridine by SPE and use of the Taguchi optimization method. Analytical Methods, 2012. 4(12): p. 4220-4229.

49. Ghasemian, M.B., et al., Lattice evolution and enhanced piezoelectric properties of hydrothermally synthesised 0.94(Bi0.5Na0.5)TiO3–0.06BaTiO3 nanofibers. Journal of Materials Chemistry C, 2017. 5(42): p. 10976-10984.

50. Ghasemian, M.B., et al., Morphology control and large piezoresponse of hydrothermally synthesized lead-free piezoelectric (Bi0.5Na0.5)TiO3 nanofibres. RSC Advances, 2017. 7(25): p. 15020-15026.

51. Ghasemian, M.B., et al., Approaching Piezoelectric Response of Pb-Piezoelectrics in Hydrothermally Synthesized Bi0.5(Na1–xKx)0.5TiO3 Nanotubes. ACS Applied Materials & Interfaces, 2018. 10(24): p. 20816-20825.

52. Heidari, M., S. Ghasemi, and R. Heidari, The Effects of Leadership and Employment in Technical Capabilities of Sport Teams. Journal of Humanities Insights, 2019. 3(02): p. 75-80.

53. Ghasemian, M.B., et al., Self-Limiting Galvanic Growth of MnO2 Monolayers on a Liquid Metal—Applied to Photocatalysis. Advanced Functional Materials, 2019. 29(36): p. 1901649.

54. Ghasemian, M.B., et al., Evidence of phase coexistence in hydrothermally synthesized K0.5Na0.5NbO3 nanofibers. Journal of Materials Chemistry A, 2020.

55. Ghasemian, M.B., et al., Peculiar piezoelectricity of atomically thin planar structures. Nanoscale, 2020. 12(5): p. 2875-2901.